Nanjing University of
Aeronautics and Astronautics

Chaotic Behaviors of an In-plane Tethered Satellite System with Elasticity

Author:	Email:
Jingtian Chen	jingtianchen@nuaa.edu.cn
Bensong Yu	yu_bensong@nuaa.edu.cn

Nanjing University of Aeronautics and Astronautics

Date: 2024.06.02

Table of Contents

1. Introduction of Tethered Satellite Systems

1.1 Background

Tethered Satellite Systems:

With an increasing number of on-orbit missions, a tethered satellite system as a novel and potential practical tool has attracted more attention from scholars.

- Low cost and reusable
- Altitude advantages of satellite deployment
- Complex space tasks can be accomplished

The Major Problem:

Modeling an orbital tethered system is a challenging problem.

- Different models were constructed.
- Simplified model qualitatively reveals global dynamic characteristics of the system.
- Sophisticated model can accurately depict dynamic behaviors.
- Two different models as well as the dynamics of tethered satellites should be analyzed due to different levels of complexity.

Fig 1. Tethered Satellite System

1. Introduction of Tethered Satellite Systems

1.2 Research Focus

- Two models of tethered satellites are developed, including the **Discrete Flexible Tether Model**, and the **Simplified Elastic Rod Model**.
- The conditions for the emergence of chaos are identified by the elastic rod model and the **Melnikov's method**.
- Global dynamics are studied, particularly the chaotic motions, of the in-plane tethered system, by using the **Cell Mapping Method**.
- Analyzing the chaos of tethered satellites with different parameters. **Numerical simulations** are used to confirm the occurrence of chaos. The parameter domains in which chaos may occur are given.

Fig 1. Tethered Satellite System

2.1 Introduction of Discrete Flexible Tether Model

A tethered satellite that moves along a circular low orbit is studied. The system under consideration consists of a mother satellite M, a sub-satellite S and a connecting flexible tether, the masses of which are m_M, m_s and m_t, respectively. The unstrained length of the elastic tether is l_0. The orbital true anomaly and orbital inclination between the equatorial and orbital planes are defined as ν and i, respectively.

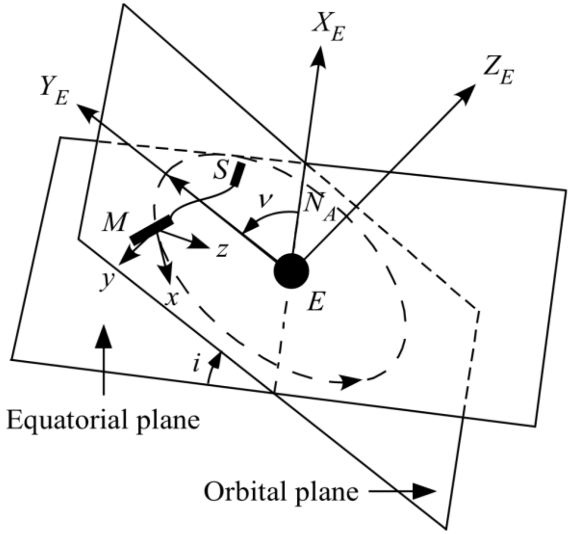

Fig 2. A two-body tethered satellite.

We assume that both satellites are slender cylinders, one end of which is connected to the space tether. (Note that different shape assumptions would lead to distinct numerical results.)

- An **in-plane pitch angle $\boldsymbol{\theta}$** for the system is defined as the angle from line $o_M E$ to line $o_M o_S$, as presented in Figure.
- An **in-plane attitude angle $\boldsymbol{\theta_{M(S)}}$** concerning the satellite rigid body is also defined as the angle from line $o_{M(S)}E$ to the axis of the cylinder.
- In addition, a particle-spring model is used to discuss the dynamics of the infinite-dimensional elastic tether.

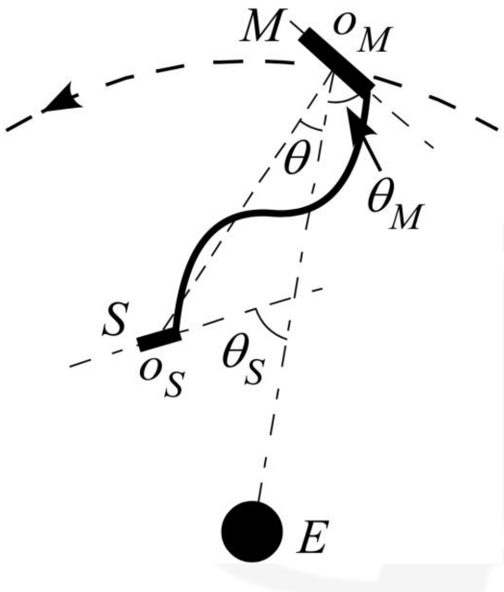

Fig 3. Definition of in-plane pitch (attitude) angle.

2.2 Discrete Flexible Tether Model

- **The dynamic equation of the mass center** of the element of the tether in the inertial coordinates $E-XEYEZ_E$ is formulated as:

$$m_k \mathbf{r}_k'' = \mathbf{G}_k + \mathbf{T}_k + \mathbf{F}_k^d (k=0,1,\cdots,n,n+1)$$

where the prime represents the derivative with respect to time t, and m_k and r_k are the mass of the node and the position vector of the node from the Earth's center E.

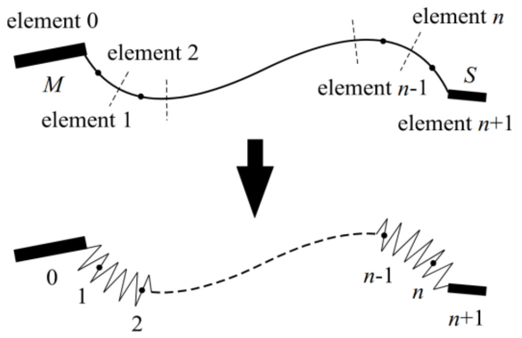

G_k: The gravity of the mass center.
T_k: The tension force from satellite (tether).
F_k^d: The air drag force.

- In order to calculate the moment balance of the system, it is necessary to analyze the gravitational moments of the nodes of the rope system.

Parameters	Explainations
μ_E	The Earth gravitational parameter
σ_U^{Masb}	The direction cosine between the coordinates and the position vector
i_e, j_e, k_e	The unit vectors of the X_E axis, Y_E axis and Z_E axis

- After calculate the principal moment vector of gravity of the mother satellite (sub-satellite) rigid body M_{iandjb}, and according to the Euler equation, **the dynamic equation of attitude** of the satellite rigid body is derived:

$$\mathbf{G}_{0(n+1)} = -\frac{\mu_E}{r_{0(n+1)}^2} \sum_{U,V,W;\mathbf{e}}^{\mathbf{i}_E \mathbf{j}_E \cdot \mathbf{k}_E} \Big\{ \Big[m_{0(n+1)} + \frac{3}{2r_{0(n+1)}^2} \left(3J_{UU}^{M(S)} + J_{VV}^{M(S)} + J_{WW}^{M(S)} - 5I - 10\tilde{I} \right) + \frac{3}{2r_{0(n+1)}^2 \sigma_U^{M(S)}} \left(2\sigma_V^{M(S)} J_{UV}^{M(S)} + 2\sigma_W^{M(S)} J_{UW}^{M(S)} \right) \Big] \sigma_U^{M(S)} \mathbf{e} \Big\}$$

$$\mathbf{J}_{0(n+1)} \omega_{0(n+1)}' + \omega_{0(n+1)} \times (\mathbf{J}_{0(n+1)} \omega_{0(n+1)}) = \mathbf{M}_{0(n+1)} + \mathbf{N}_{0(n+1)}$$

$\mathbf{N}_{iandjb}$ is the moment from the resultant external force.

2.3 Elastic Rod Model

The sophisticated discrete model can more accurately describe the dynamics of the original system, but may not predict global dynamic characteristics.

- The dynamic equation of the orbital system in a nondimensional form:

$$\ddot{\theta}+2\widehat{m}(\dot{\theta}+1)\frac{\dot{\varepsilon}}{1+\varepsilon}+3\sin\theta\cos\theta=\frac{Q_d}{\widetilde{m}l_0^2(\mu_E/r_c^3)}$$

- Using the torque formula and the principle of virtual work.
- Based on a straightforward application of the second Lagrange equation.
- θ is the generalized coordinate.
- The dynamic equation of the orbital system in a nondimensional form is:

$$\ddot{\theta}+3\sin\theta\cos\theta=\gamma\cos^2\theta+\mu(\dot{\theta}+1)\sin\omega_\varepsilon\nu$$

$$\gamma=\sum_{j=M,S,t}(C_{d,j}\rho_{a,j}\kappa_j)\frac{r_c^3\left(\sqrt{\mu_E/r_c}-\omega_E r_c\cos i\right)^2}{\mu_E\widetilde{m}l_0}\ and\ \mu=2\widehat{m}a_\varepsilon\omega_\varepsilon$$

It is a simplified model of the tethered satellite system in the orbital plane.

- A tether with microamplitude longitudinal oscillation is modeled **as a uniform elastic straight rod** of current length $l = l_0(1+\varepsilon)$, where $|\varepsilon| \ll 1$ is the longitudinal strain.
- Two satellites are viewed as cylinders, whose axes are always parallel to the tether.

Parameters	Definitionss
$\hat{m}=m_M(m_S+m_t/2)/(\tilde{m}\bar{m})$	Reduced system masses 1
$\tilde{m}=[(m_M+m_t/2)(m_s+m_t/2)]/\bar{m}-m_t/6$	Reduced system masses 2
$\bar{m}=m_M+m_S+m_t$	Total system mass
r_c	distance between the center of mass of the system and the center of the Earth
$\epsilon=\epsilon_0+a_\epsilon\cos\omega_\epsilon\upsilon$	Strain
ϵ_0	Static strain
a_ϵ	Amplitude
υ	Non-dimensional time

Table 2. Definitions of Parameters in Model

3.1 Chaos Near Heteroclinic Points

- Describe how chaotic behaviors are identified in a nonautonomous two-dimensional system (**Elastic Rod Model**).
- Starting with the unperturbed Hamiltonian system, unstable equilibrium points and analytical heteroclinic orbits can be solved.
- As a necessary condition, the Melnikov method is used to analyze whether chaotic behaviors occur.
- Chaos might appear near heteroclinic points if the conditions solved by Melnikov method are satisfied.

How to identify the chaos?
For the perturbed system, an invariant set that results in chaos is more likely to emerge **if the stable and unstable manifolds intersect transversally in the vicinity of the saddle points.**

Unstable Equilibrium Points $P_{1,2}$: $(\mp \pi/2, 0)$

$$\Gamma_{1,2}: \theta^h(\nu) = \begin{bmatrix} \theta_1^h(\nu) \\ \theta_2^{h\pm}(\nu) \end{bmatrix} = \begin{bmatrix} \operatorname{arcsintanh}\sqrt{3}\nu \\ \pm\sqrt{3}\operatorname{sech}\sqrt{3}\nu \end{bmatrix}, \theta_1^h \in [-\pi/2, \pi/2]$$

$$\Gamma_{3,4}: \theta^h(\nu) = \begin{bmatrix} \theta_1^h(\nu) \\ \theta_2^{h\pm}(\nu) \end{bmatrix} = \begin{bmatrix} \operatorname{arcsintanh}\sqrt{3}\nu \pm \pi \\ \pm\sqrt{3}\operatorname{sech}\sqrt{3}\nu \end{bmatrix}, \theta_1^h \in \left[-\pi, -\pi/2\right) \cap \left(\pi/2, \pi\right)$$

Heteroclinic Orbit

$$M(\nu_0) = \int_{-\infty}^{+\infty} \theta_2^{h\pm}(\nu)\left[\gamma\cos{}^2\theta_1^h + \mu\left(\theta_2^{h\pm}+1\right)\sin\omega_\varepsilon(\nu+\nu_0)\right]\mathrm{d}\nu$$

$$\left|\frac{\gamma}{\mu}\right| < 2\omega_\varepsilon \operatorname{csch}\frac{\omega_\varepsilon \pi}{2\sqrt{3}} \pm 2\operatorname{sech}\frac{\omega_\varepsilon \pi}{2\sqrt{3}}$$

Melnikov Function

- This equation implies that the sign of $M(\nu_i)$ changes for a sufficiently small perturbation, so that **the stable and unstable manifolds intersect transversally at heteroclinic points**. Therefore, chaos might appear near heteroclinic points.

3.2 Simulation Results and Analysis

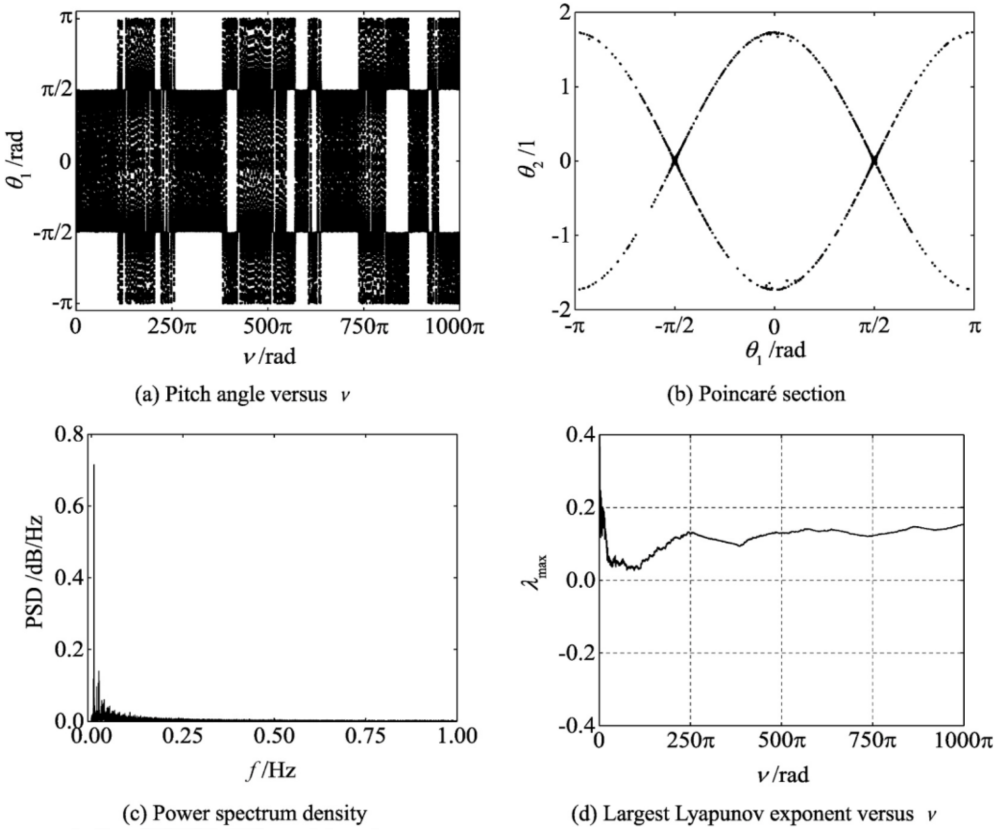

Fig 4. Chaotic motion induced by microamplitude oscillation and atmospheric drag

H = 820 km, $\omega_{\varepsilon z}$ = 5000 $\sqrt{\mu_e / r_c^{1}}$ aε = 1 × 10 4

the parameter ratio: |γ /μ| = 0.0015 < 0.1528

Chaos Occur!

Dynamic behavior depicted in the figure:

- Irregular in-plane pitch motion as true anomaly υ varies (Fig. 4(a)).
- The Poincaré section of trajectories shows numerous transverse heteroclinic points near unstable saddle points (Fig. 4(b)).
- Power Spectrum Density (PSD) in Fig. 4(c) exhibits a significant power spectrum in the frequency range f∈[0, 0.25].
- Change in largest Lyapunov exponent λmax with v illustrated in Fig. 4(d), consistently above 0.

Parameters	Explainations
m_M=500 kg m_S=50 kg, m_t=0.5 kg	Masses of the satellites and tether
l_{i}=10 km, d_t=0.5x10³ m	The unstrained length and diameter of the tether
$C_{deMasetb}$=2.2	The drag coefficient of the satellites (tether)
A_M = 1.0m², A_S = 0.1m²	The representative areas of the satellites
i = π/4	The orbital declination

3.2 Simulation Results and Analysis

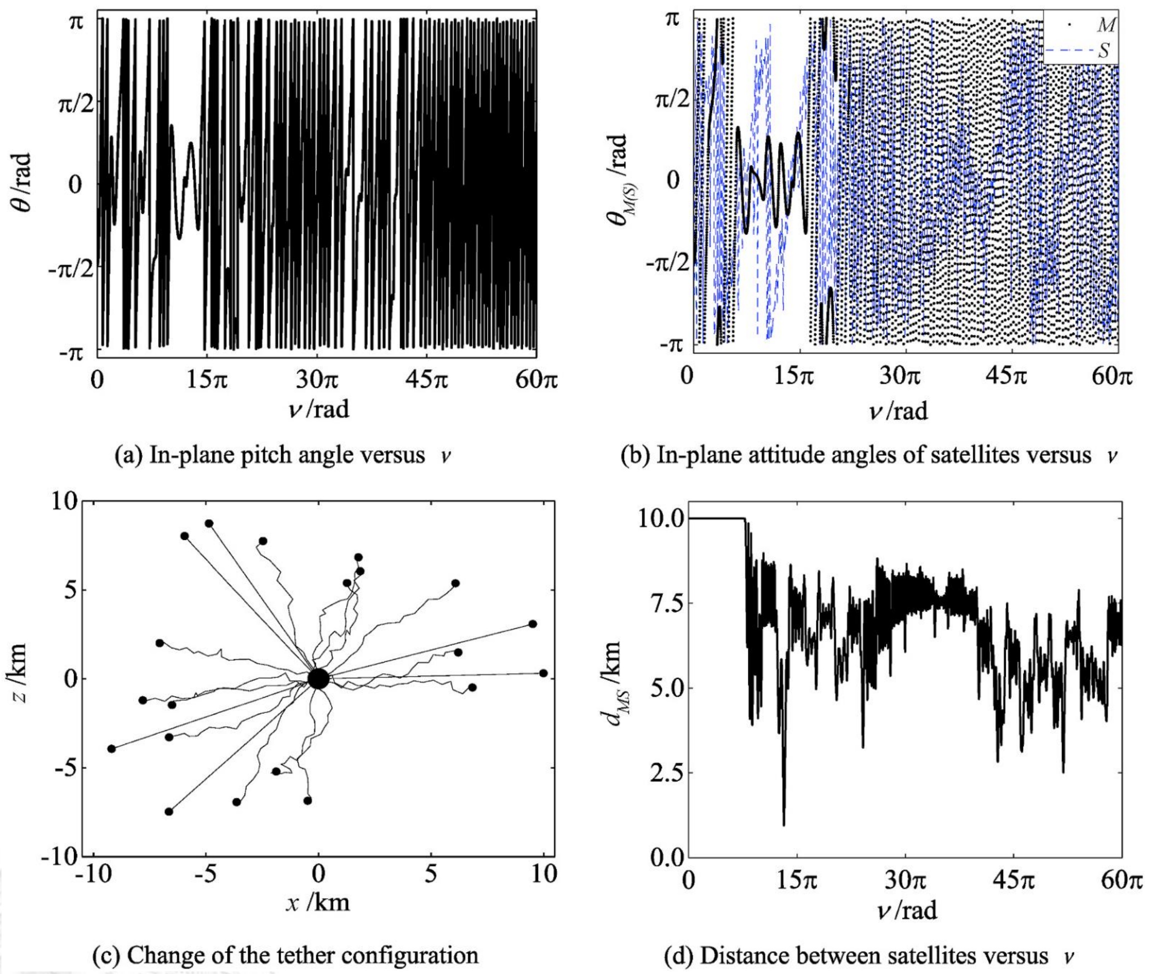

Fig 5. Chaotic motion based on the sophisticated discrete model.

- Utilization of discrete tether model to verify chaotic motion.
- Space tether, EA = 10^7 N, divided into 20 uniform elements.
- Variation in in-plane pitch angle with true anomaly ν displayed in Fig. 5(a), showing alternating, non-periodic pendulum-like and spinning motions.
- The time history of coupling in-plane attitude angles of satellites is shown in Fig. 5(b), indicating intense irregular oscillations.
- Configuration change of flexible tether depicted in Fig. 5(c).
- Distance between the mother satellite and sub-satellite (d_{MS}) illustrated in Fig. 5(d), indicating tether slackness due to atmospheric drag and microgravity field.
- Results consistent with elastic rod model results.

3.2 Simulation Results and Analysis

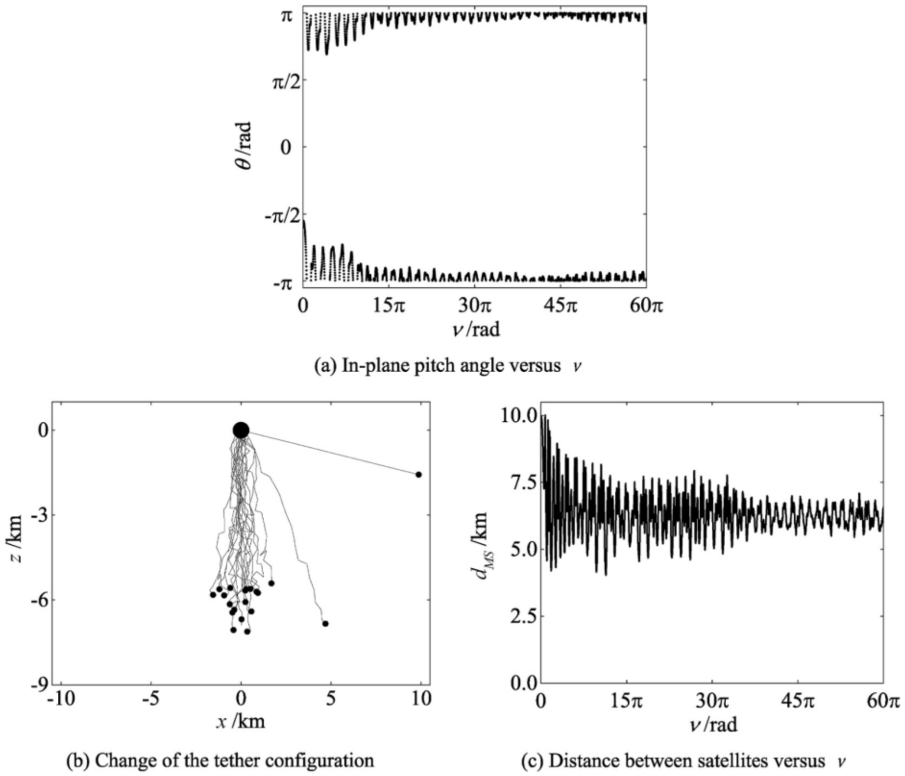

Fig 6. Dynamics of the system based on the particle-spring model.

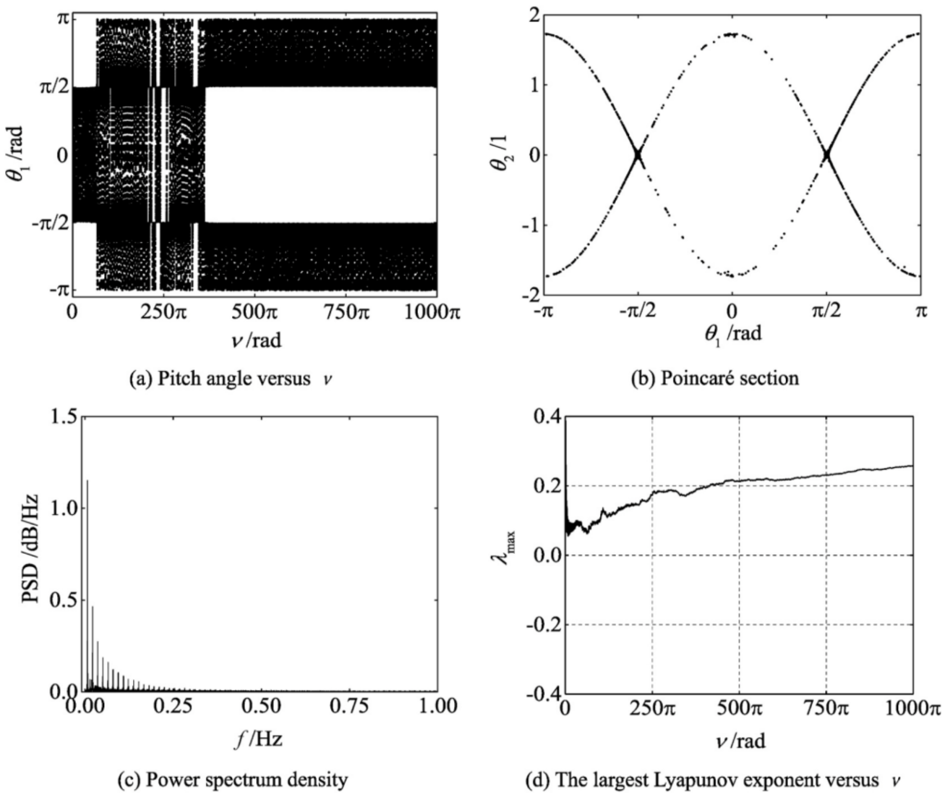

Fig 7. Dynamics of the system without rigid body attitudes.

Discussion on the impact of satellite attitudes on dynamics.

- Representative areas of two satellites: $A_M = 0$, $A_S = 0$ (viewed as mass points).
- Stable pendulum-like motion retained after transient chaos in Fig. 7.
- The dynamic behaviors on the basis of a particle-spring model are compared in Fig. 6, where the chaotic motion also disappears.

Conclusion: System dynamics are sensitive to the rigid body attitudes of satellites.

3.2 Simulation Results and Analysis

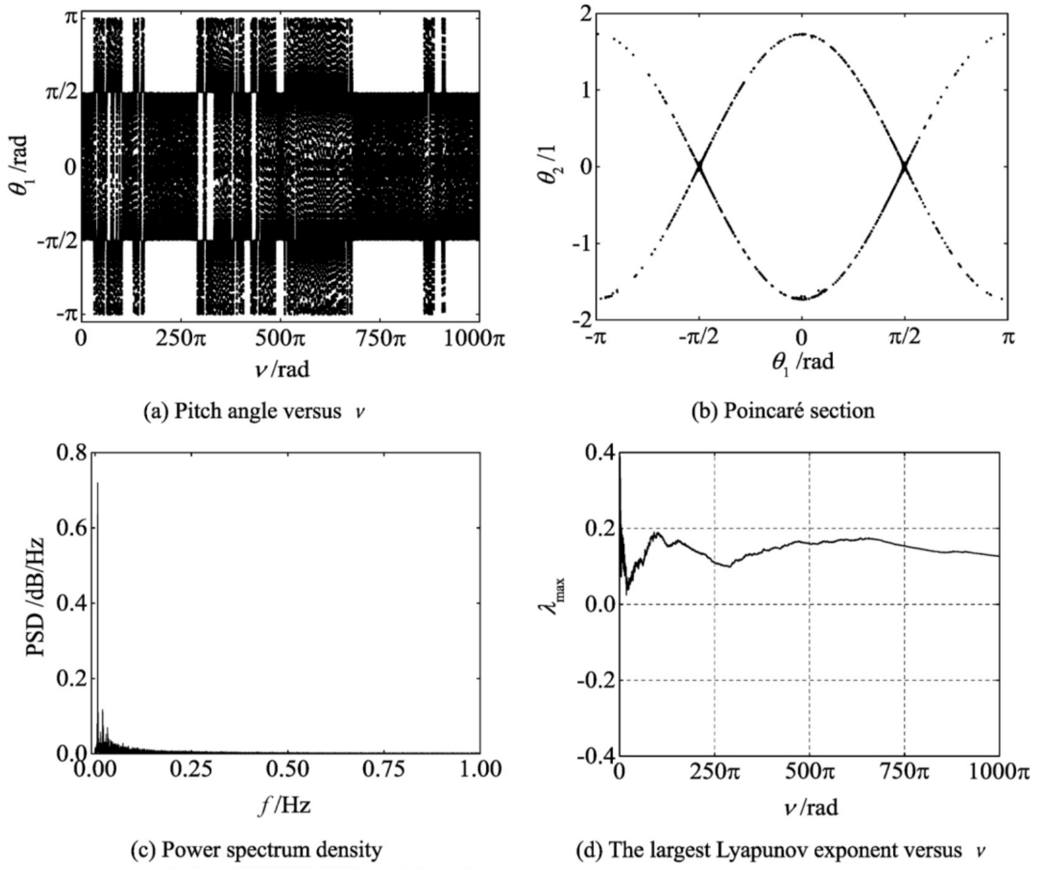

Fig 8. Effect of the mass distribution on the dynamics.

Alteration of sub-satellite mass to m_S = 25 kg.

- The influence of mass distribution on system dynamics is presented.
- Chaotic motion is significantly different from Fig. 4.

Conclusion: **Dynamic behavior is governed by the mass distribution of the system.**

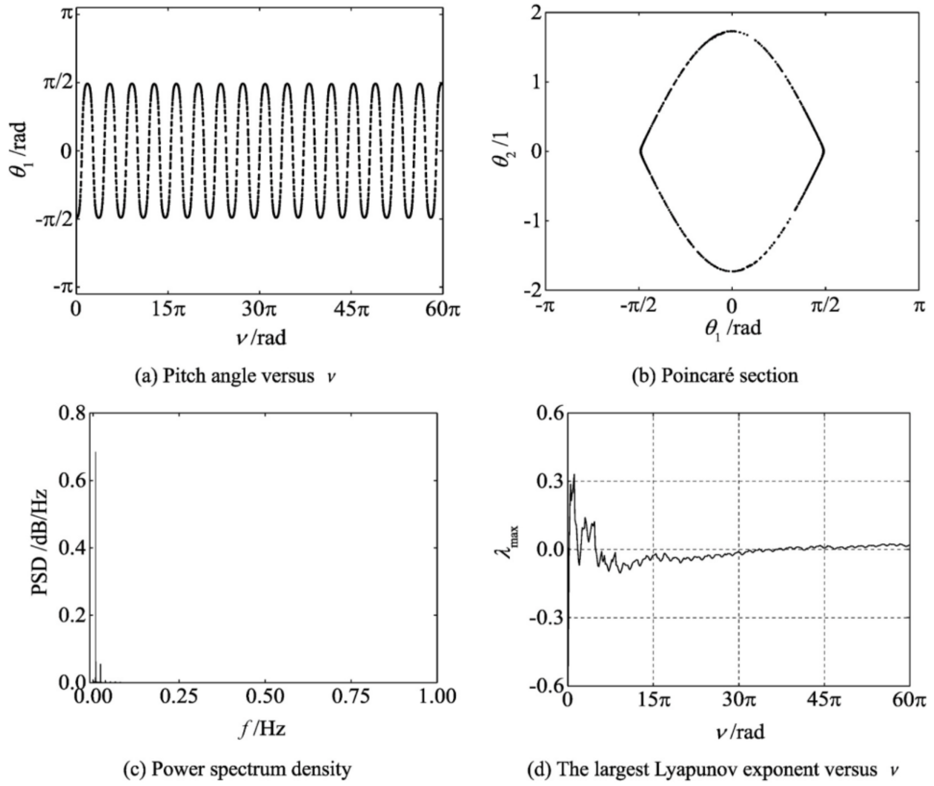

Fig 9. Effect of the tether length on the dynamics.

Reset unstrained tether length to l_0 = 7.5 km.

Inference of pendulum-like oscillation from pitch angle change.

- Characteristics indicating quasi-periodic motion.
- Peaks in power spectral density (PSD).
- Largest Lyapunov exponent approaching 0.
- Criterion $|\gamma / \mu| = 0.0016 < 0.1528$ met, but chaotic motion absent.

Conclusion: **Dynamics affected by tether length.**

3.3 Global Dynamics Analysis

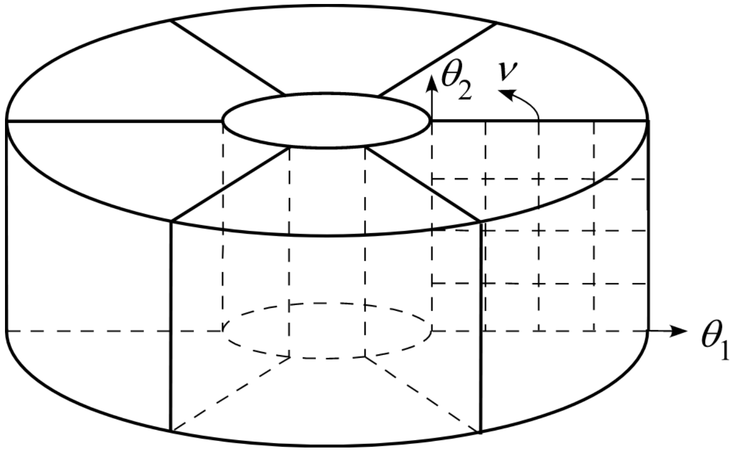

Fig 10. Division of the cell element.

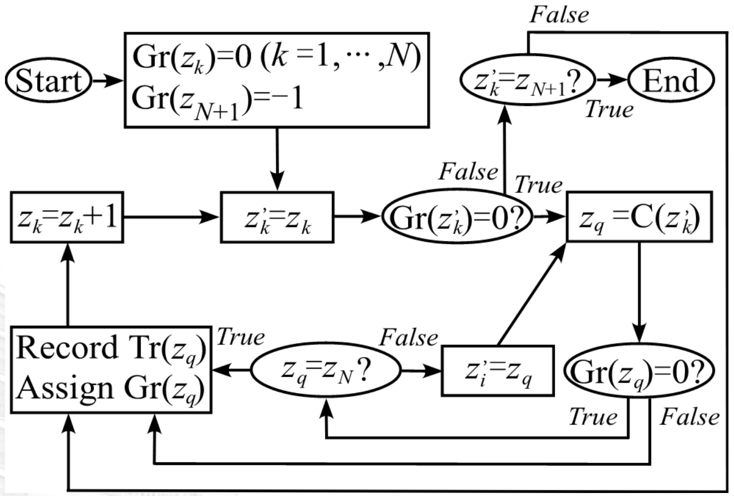

Fig 11. Sketch chart of the cell mapping algorithm.

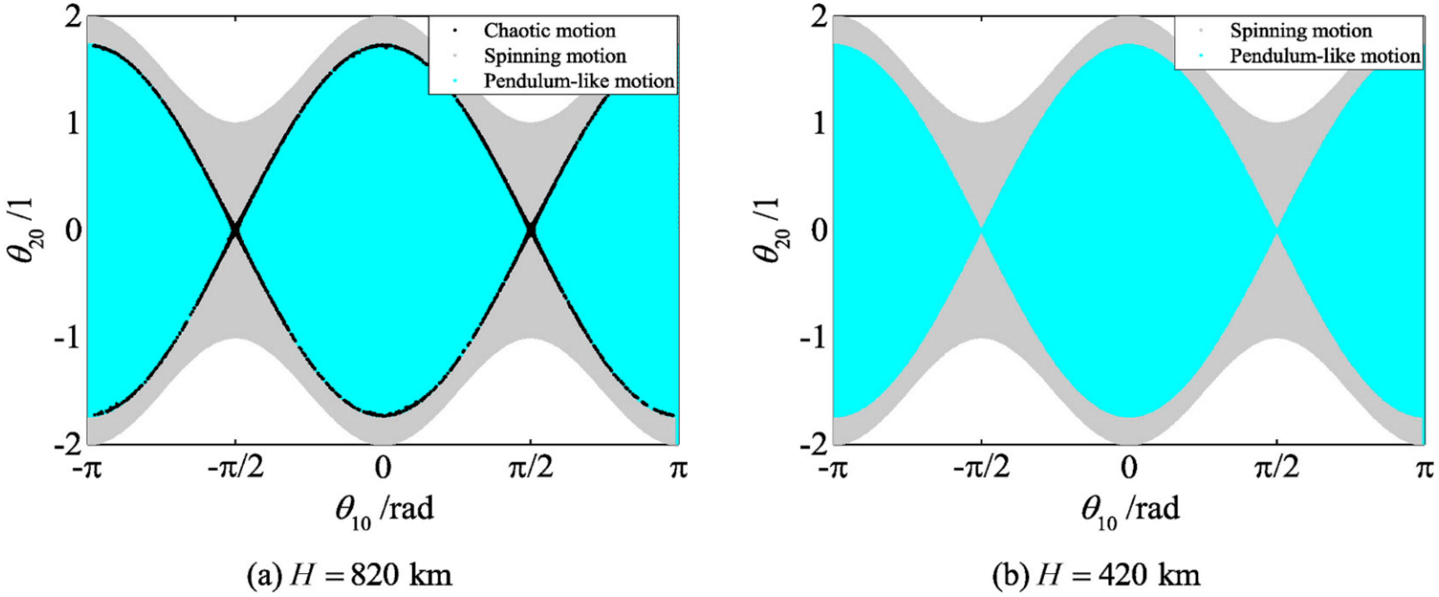

Fig 12. Global dynamics.

- **The orbital altitude reaches H = 820 km, chaotic motion, spinning motion, and pendulum-like motion occur, as shown in Fig. 12(a).**
- **The initial states near the unstable saddle points and heteroclinic orbits might lead to chaotic motion.**
- **The white zone corresponds to cells that eventually fall into the sink cell due to variable ranges.**
- **The finite cell elements actually do not depict ergodicity in chaos; thus, this motion is only strictly identified as irregular.**
- **The chaotic motion will disappear once the orbital altitude decreases to H = 420 km because the system parameters do not satisfy the inequality.**

4. Discussions and Conclusions

Chaotic behaviors in nonautonomous two-dimensional tethered satellite systems are revealed.
Chaos occurs when stable and unstable manifolds intersect transversally.
A critical ratio of perturbation parameters is provided.
Numerical results show:

- Higher orbital altitude and larger amplitude contribute to chaos.
- Dynamics depend on parameters like satellite attitudes, mass distribution, and tether length.
- A flexible tether model is structured in the form of discrete elements to verify the chaotic motion that appears in an elastic rod model.
- Conclusion: Perturbations may induce chaos in tethered satellites.

Chaotic behaviors of an in-plane tethered satellite system with elasticity

Thank You For Listening!

Question Time